

# RSC Advances



This is an *Accepted Manuscript*, which has been through the Royal Society of Chemistry peer review process and has been accepted for publication.

*Accepted Manuscripts* are published online shortly after acceptance, before technical editing, formatting and proof reading. Using this free service, authors can make their results available to the community, in citable form, before we publish the edited article. This *Accepted Manuscript* will be replaced by the edited, formatted and paginated article as soon as this is available.

You can find more information about *Accepted Manuscripts* in the [Information for Authors](#).

Please note that technical editing may introduce minor changes to the text and/or graphics, which may alter content. The journal's standard [Terms & Conditions](#) and the [Ethical guidelines](#) still apply. In no event shall the Royal Society of Chemistry be held responsible for any errors or omissions in this *Accepted Manuscript* or any consequences arising from the use of any information it contains.

Cite this: DOI: 10.1039/c0xx00000x

www.rsc.org/xxxxxx

ARTICLE TYPE

## Tunable hydroxylated surfactants: An efficient toolbox towards anisotropic gold nanoparticles

Monique Gabriella Angelo da Silva<sup>a,b</sup>, Mario Roberto Meneghetti<sup>b</sup>, Audrey Denicourt-Nowicki<sup>a\*</sup>, and Alain Roucoux<sup>a\*</sup>

Received (in XXX, XXX) Xth XXXXXXXXXX 20XX, Accepted Xth XXXXXXXXXX 20XX  
DOI: 10.1039/b000000x

**Easily tunable *N,N*-dimethyl-*N*-alkyl-*N*-(HydroxyAlkyl) Ammonium salts have been synthesized and used as capping agents to produce size- and shape-controlled anisotropic gold nanoparticles. The influence of the lipophilic chain length and the counter-ion of this original library of hydroxylated surfactants has been evaluated. From this study, various shapes (spheres, rods, prisms) have been achieved.**

Anisotropic gold nanoparticles (AuNPs) have received widespread attention in the last decades, owing to their unusual shape- and size-dependent physical and chemical properties, including optical and electronic responses<sup>1-4</sup> or catalytic activity.<sup>5-6</sup> For example, spherical AuNPs present one plasmon absorbance of similar energies whatever the size. On the contrary, one of the most outstanding features of gold nanorods (AuNRs) remains the presence of two plasmon bands in the UV-vis-NIR absorption spectrum, and more especially the longitudinal plasmon which is strongly dependent of the aspect ratio.<sup>7-8</sup> These nanomaterials, possessing shape- and size-dependent properties, have found numerous applications in sensing,<sup>9-10</sup> diagnostics,<sup>11</sup> photothermal therapy for cancer.<sup>12-13</sup> For catalytic applications, anisotropic nanoparticles could provide a promising tool to tune the catalytic activity through the availability of high index facets that could facilitate adsorption and surface reactions.<sup>14-17</sup> In that context, the optimization of the AuNPs performances for a given application relies on the production of AuNPs with precisely designed physico-chemical properties, and a rigorous control of the shape (aspect ratio) and the dimensions (length and diameter).<sup>18-21</sup> Among the various synthetic approaches,<sup>22</sup> the seeded-growth methodology proved to be the most versatile to produce AuNPs with quite decent yields and sample monodispersity,<sup>23-24</sup> given rise to a vast library of nanostructures ranging from octahedra or cubes,<sup>24-25</sup> to prisms<sup>26-27</sup> or to original nanostructures with high index facets.<sup>28-30</sup> Various surfactants, and more particularly quaternary ammonium salts, have been used as capping agents to achieve a good shape control over the nucleation and growth of AuNPs, owing to their dual role. First, these compounds are efficient capping agents, adsorbing on gold surface in a bilayer fashion and thus avoiding undesirable agglomeration. Secondly, they could promote specific interactions within the particle facet, thus influencing the growth

kinetics and thereby the morphology of nanospecies.<sup>17</sup> Until now, cetyltrimethylammonium bromide (CTAB) remains the most widely used and the influence of several structural parameters,<sup>31</sup> such as the hydrophobic chain length,<sup>32-33</sup> the counter-ion<sup>33-34</sup> and the impurity ions present in the cationic surfactants,<sup>27</sup> have been studied. To our knowledge, only a few works have been reported to the potential impact of the surfactant head group and their functionalisation. In 2006, Wang *et al.*<sup>35-36</sup> have explored the effect of the surfactant headgroup size on the growth of gold nanostructures, comparing various cetyltrialkylammonium bromides. More recently, our group reported a new family of easily tunable *N,N*-dimethyl-*N*-cetyl-*N*-(HydroxyAlkyl) Ammonium bromide salt (HAA16Br), bearing an hydroxylated polar head with various lengths from ethoxy (HEA) to butoxy (HBA) groups, as efficient driving agents.<sup>37</sup> We have demonstrated that the presence of the hydroxyl group was beneficial to promote headgroup packing at the metal surface, thus leading to the formation of rod-like particles of tunable aspect ratios.

Herein, we extend the library of hydroxylated ammonium salts for the production of size and shape-controlled gold NPs in high yields and selectivities. New *N,N*-dimethyl-*N*-alkyl-*N*-(hydroxyalkyl) ammonium salts (HAAX) were investigated as capping agents in anisotropic gold nanoparticle synthesis by the seed-mediated growth in aqueous media (Fig. 1).

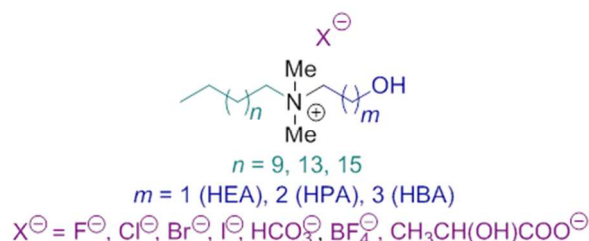


**Fig.1** General chemical of *N,N*-dimethyl-*N*-alkyl-*N*-(HydroxyAlkyl) Ammonium salts (HAAX) surfactants as NPs growth-driving agents

In addition to the length of the polar head,<sup>37</sup> several structural parameters have been studied, such as the length of the lipophilic

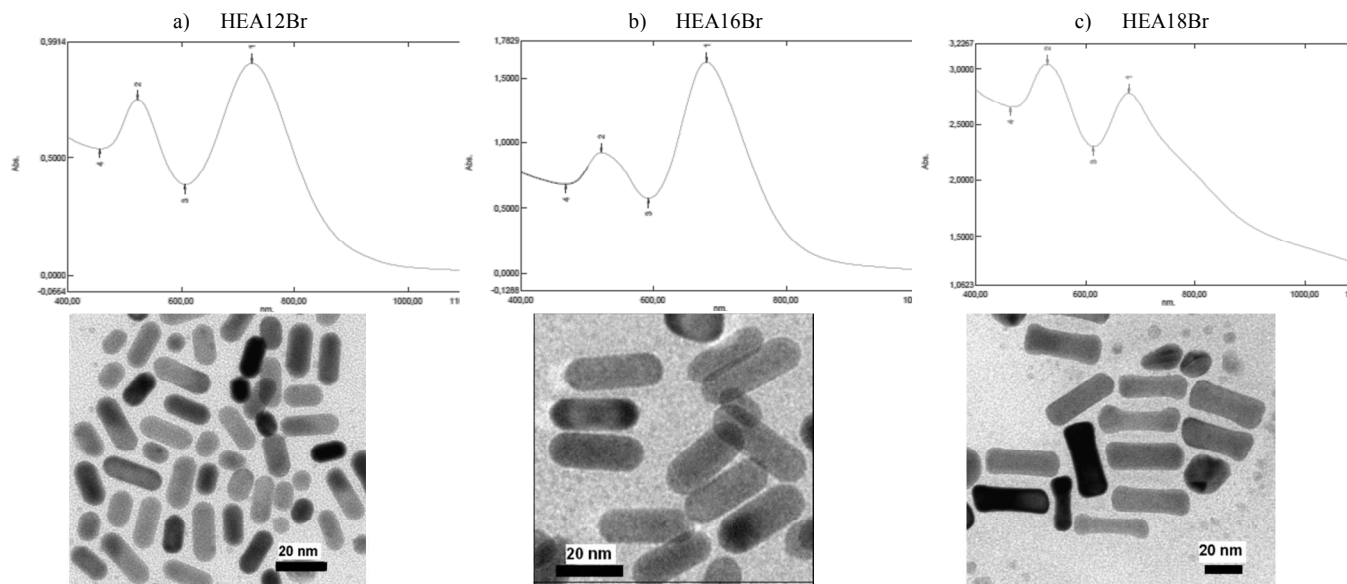


Fig.2 UV-vis absorption spectrum and TEM picture of AuNRs obtained with a) HEA12Br (19 x 8 nm, aspect ratio of 2.4,  $\lambda_{\max} = 724$  nm), b) HEA16Br (30 x 10 nm, aspect ratio of 3.0,  $\lambda_{\max} = 679.50$  nm), c) HEA18Br (45 x 14 nm, aspect ratio of 3.2,  $\lambda_{\max} = 678$  nm). Size and aspect ratio were obtained after 500 counts for each sample. Scale bar = 20 nm

chain (C12, C16, C18),<sup>38</sup> ii) the nature of the counter-ion through an anionic metathesis reaction ( $X^- = F^-, Cl^-, Br^-, I^-, BF_4^-, HCO_3^-$  and lactate).<sup>39-40</sup> Based on several sets of experiments, we report in this manuscript how to produce anisotropic gold nanoparticles with well-controlled morphologies according to an easy chemical modification of the surfactant and not just as an addition of the corresponding salt in the mixture

## Results and discussion

In this study, AuNPs were synthesized by the seeded-growth methodology in aqueous media, using *N,N*-dimethyl-*N*-alkyl-*N*-(hydroxyethyl)ammonium salts (HEAX), bearing a hydroxyethyl polar head, various lengths for the lipophilic chain (C12 to C18) and counter-ions ( $X^- = F^-, Cl^-, Br^-, I^-, BF_4^-, HCO_3^-$  and lactate), as capping agents. The syntheses were performed in the presence of silver nitrate  $AgNO_3$ . The selectivity was determined, without centrifugation step, as the number of AuNPs in a well-defined shape over the number of NPs from Transmission Electron Microscopy (TEM).

In a first set of experiments, we investigated the influence of the length of the lipophilic chain (C12, C16, C18) on the particle morphology, considering a 2-hydroxyethylammonium (HEA) polar head and a bromide as counter ion. These surfactants were easily prepared by quaternarization of *N,N*-dimethylethanolamine with the appropriate bromoalkane (see Supporting Information). The results were compared to those obtained with the classical cetyltrimethylammonium bromide (CTAB) under the same preparation conditions. Figure 2 shows the UV-vis absorption spectra and TEM images of AuNPs prepared by the seeded-growth method, as a function of the different chain lengths for *N,N*-dimethyl-*N*-alkyl-*N*-(hydroxyethyl)ammonium bromide salts (HEAnBr, with  $n = 12, 16, 18$ ).

As already observed with various CTAB analogues of various lengths for the hydrocarbon tail, the lipophilic chain seems to influence the AuNPs morphology and higher aspect ratio

nanorods were produced while increasing the chain length. With a small lipophilic chain (HEA12Br), the growth control seems not very efficient, leading to a mixture of spherical particles (~ 10 nm) and low aspect ratio (2.4) nanorods with selectivity about 78% (Fig. 2a). In the case of HEA16Br, as previously reported,<sup>37</sup> the UV-vis absorption spectrum of AuNPs presents two typical absorption bands with a good correlation, suggesting the formation of nanorods (Fig. 2b). This result was confirmed by TEM analyses, showing rod-like particles with an aspect ratio of 3.0 (30 x 10 nm) with a high selectivity of 88%. This surfactant, possessing a higher water-solubility thanks to the hydroxylated polar head in comparison with CTAB derivatives, is easily synthesized in good yields and could be used in a large range of concentration if needed in nanoparticles synthesis. For comparison, the aspect ratio of AuNRs obtained with CTAB by the same procedure is around 3.3 (40 x 12 nm), similar to the values reported in the literature.<sup>37, 41</sup> The hydroxyalkylammonium bearing an alkylchain with 18 carbons (HEA18Br) was also evaluated as directing agent, but it is difficult to compare the result, owing to the use of less concentrated surfactant solution (See experimental section). However, dog-bone shape particles, which could find promising applications, leading to a red-shift,<sup>42</sup> were mainly produced (Fig. 2c), probably owing to an insufficient amount of capping agents. It is also worth mentioning that without a hydroxyethyl substituent on the nitrogen atom, only few anisotropic AuNPs are produced due to the low water solubility of the capping agent. Moreover, the aspect ratios are lower than those observed by Murphy et al. using CTAB analogues with different lipophilic chains,<sup>32</sup> since only the initial step of the seed-mediated growth process was explored in this study. To resume, the highly water-soluble HEA16Br salt seems to be a good compromise to achieve pertinent aspect ratios, assuming an efficient binding of  $Au^{III}$  and  $Au^I$  ions into the cationic micelles present in solution,<sup>43</sup> as well as the van der Waals stabilization of the surfactant bilayer on gold surface owing to the interchain packing of the hydroxylated head group,

which helps the underlying nanorod formation.<sup>32</sup>

In a second set of experiments, the influence of the counter-ion on the particle formation was studied, considering the role of the counter-ions adlayers in the control over the shape development in the growth from a crystal seed.<sup>33, 44</sup> Various HEA16X ( $X^- = F^-, Cl^-, Br^-, I^-, BF_4^-, HCO_3^-$  and Lactate), bearing a lipophilic chain of 16 carbons and a 2-hydroxyethyl ammonium polar head, were easily synthesized by quaternization of *N,N*-dimethylethanolamine with the appropriate halogenoalkane ( $X^- = Cl^-, Br^-, I^-$ ),<sup>45</sup> or by anionic metathesis from HEA16Br.<sup>40</sup> They were evaluated as capping agents of AuNPs, in the presence of silver nitrate. First, although these counter-ions are original in gold nanoparticles synthesis, HEA16BF<sub>4</sub> and HEA16Lactate were not pertinent as capping agents, due to their quite low water-solubility and thus their aggregation even in more diluted concentrations. Secondly, the colloids prepared with HEA16F and HEA16Cl displayed only one absorption band in their respective UV-vis spectra (Fig. 3a and 3b), suggesting the formation of spherical particles, as assessed by Transmission Electron Microscopy pictures. The spherical AuNPs capped with HEA16F (8.5 nm) are smaller than those obtained by HEA16Cl (10 nm). Similar observations have already been reported by Kawasaki et al.,<sup>33</sup> with spherical AuNPs obtained by hydrazine reduction in the presence of CTAF and CTACl, and was attributed to a fast reduction rate promoting by the use of a fluoride salt. On the contrary, two absorption bands were observed in the UV-vis absorption spectra of colloids synthesized from the newly HEA16HCO<sub>3</sub> salt (Fig. 3c) as well as HEA16Br (Fig. 2b), being consistent with the Au nanorods observed by TEM analyses. This shape tendency of AuNPs according to the counter-ion species may be attributed to the adsorption affinity of the surfactant anion on gold surface during the crystal growth.<sup>46</sup> A similar tendency has already been observed with CTAX salts, and was correlated with the decrease in the frequency shift of Quartz Crystal Microbalance (QCM) in the following order:  $Br^- > Cl^- > F^-$ .<sup>33, 46</sup> Thus, the fluoride and chloride anions generate weak interactions within the particle surface, thus disfavoring the formation of a stable and compact double layer of the surfactant

around the growing particle, while the high-affinity adsorption of Br<sup>-</sup> onto Au surfaces produces anisotropic gold nanoparticles. Moreover, in the synthetic method used, silver ions are also introduced into the reaction, and thus the influence of halides on crystal growth are more complex since the halides interact with the Au ions in solution and the gold surface, and also with the silver ions in solution. In fact, Mirkin et al.<sup>19</sup> have found that in the presence of larger halides, the stability of the underpotentially deposited silver layer decreases, owing to the increasing strength of the Au-halide interaction relative to the Ag-Au and Ag-halide interaction.

In the particular case of HEA16HCO<sub>3</sub> salt, we could presume that, by analogy to carboxylate anions or polycarboxylates, such as citrate polyanions, the hydrogenocarbonate counter-ion provides an intermediate adsorption affinity at the growing NP surface, between the bromide and the chloride ones. However, a poor relationship between the two typical absorption bands was observed, which could be attributed to a less efficient control of the NPs growth, as confirmed by TEM images with the formation of peanut pod shape AuNPs (Fig. 3c).

Finally, the iodide counter-ion plays a critical role in the growth control of Au nanocrystals, with mainly the formation of well-formed nanoprisms (41%) as shown by TEM analyses (Fig. 3d) even if other morphologies (spheres, penta-twinned crystals) were observed (See ESI Fig. 7). This counter-ion is known to promote the formation of nanoprisms by preferential binding to <sup>9</sup> facet of gold nanocrystal with binding energies that follows the ion polarizability ( $I^- > Br^- > Cl^-$ ) and crystal facet ( $\{111\}^{22} > \{110\} > \{100\}$ ).<sup>47</sup> This effect of iodide on the shape of AuNPs have already been described with low concentrations (< 3.0 ppm) of iodide impurities present in CTAB<sup>27, 48</sup> or with the deliberate addition of potassium iodide in the presence of CTAB.<sup>19, 44</sup> These gold triangular nanoprisms are promising materials with applications in optics and electronics,<sup>49</sup> and as biosensing platforms.<sup>50</sup>

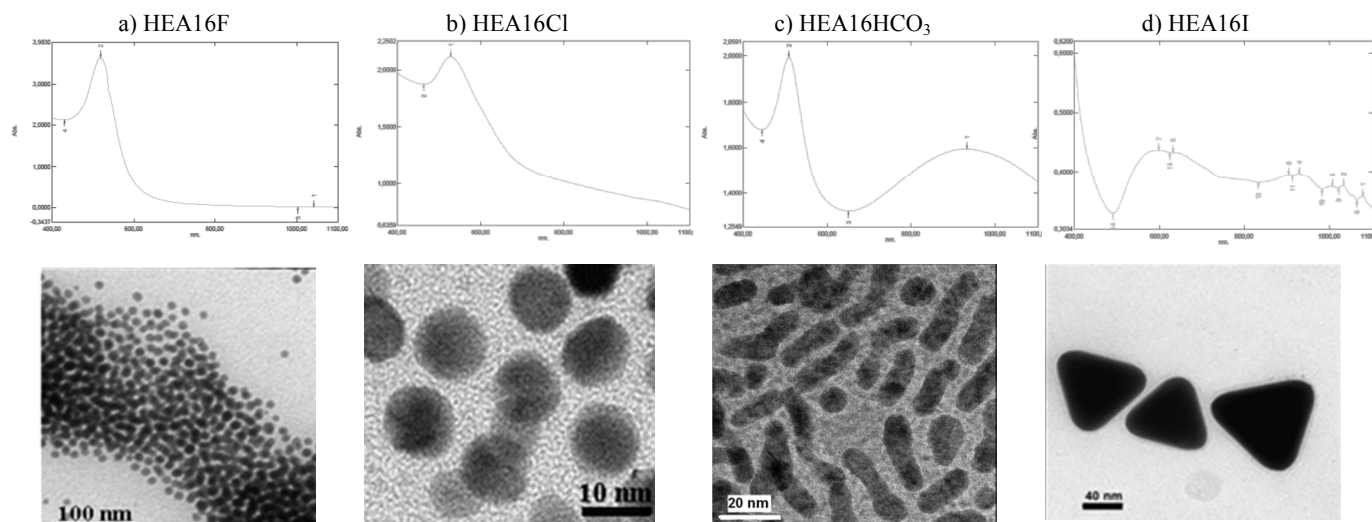


**Fig.3** Influence of the surfactant counter-ion on the morphology of AuNPs - UV-vis absorption spectra and TEM pictures of a) HEA16F (spherical NPs, 8.5 nm, Scale bar = 100 nm), b) HEA16Cl (spherical NPs, 10 nm, Scale bar = 10 nm), c) HEA16HCO<sub>3</sub> (worm-like NPs, 29 x 7 nm, aspect ratio = 4.2,  $\lambda_{max} = 932$  nm, Scale bar = 20 nm), d) HEA16I (prisms NPs, Scale bar = 40 nm). Size and aspect ratio were obtained after 500 counts for each sample.

## Conclusions

In summary, a novel library of easily tunable hydroxylated ammonium surfactants were synthesized and used as versatile growth driving agents of AuNPs. This original family provides more flexible shape templates than the CTAB, giving rise to AuNPs of various morphologies (rods, spheres, prisms.....) and different sizes through the easy modulation of the capping agent (length of the lipophilic chain, or of the polar head, and the counter-ion), with good yields and selectivities without size/shape selection step. These promising results open new perspectives in the design of original growth driving agents to produce anisotropic gold nanoparticles with well-controlled morphologies and dimensions according to the desired application, in aqueous solution without any mixture with CTAB or addition of different additives as ions and solvents.

## Experimental section

### General

Tetrachloroauric acid hydrate,  $\text{HAuCl}_4 \cdot \text{H}_2\text{O}$  (99.9%), sodium borohydride, (+)-L-ascorbic acid (99%), CTAB and  $\text{AgNO}_3$  (99%) were used as purchased, without any purification. The *N,N*-dimethyl-*N*-alkyl-*N*-(HydroxyAlkyl)Ammonium salts (HAAX) were synthesized and characterized by Mass and NMR spectroscopy (data are presented in the supplementary information).<sup>38, 43</sup> Distilled water was used to prepare all solutions. UV-Vis/near-IR spectra were recorded on a Shimadzu UV-vis 1800 spectrophotometer, using optical glass cells with length of 1 cm. The set-up was configured to fix the baseline of distilled water absorption band from 400 to 1000 nm. TEM analyses were performed on a JEOL TEM 100CXII electron microscope at an accelerating voltage of 100 kV. The samples were prepared by the addition of a drop of the gold colloidal solution on a copper grid coated with a porous carbon film. TEM images and determined selectivity were obtained from the produced gold suspension of particles without treatment such as centrifugation.

### Seed-mediated growth synthesis

AuNPs prepared in this study were produced by a seeded-growth method, adapted from the protocols developed by Murphy<sup>7</sup> and El Sayed.<sup>21</sup> The method consists in preparing two solutions: i) the seed solution and ii) the growth solution.

**Seed solution:** In a 25 mL-flask, 0.1 mL of an aqueous solution of  $\text{HAuCl}_4 \cdot 3\text{H}_2\text{O}$  ( $0.025 \text{ mol.L}^{-1}$ , 0.0025 mmol) was added to a 7.4 mL aqueous solution of surfactant ( $0.0676 \text{ mol.L}^{-1}$ , 0.5 mmol) (in the case of HEA18Br, a 7.4 mL aqueous solution of surfactant ( $0.0337 \text{ mol.L}^{-1}$ , 0.25 mmol) was used). Then, under stirring, 0.6 mL of an ice-cold aqueous solution of sodium borohydride ( $0.01 \text{ mol.L}^{-1}$ , 0.006 mmol) was added. The solution color immediately turned to brown. After 2 min, the system remains at least 2 h, without stirring before used.

**Growth Solution:** In a 25 mL-flask, 0.2 mL of an aqueous solution of  $\text{HAuCl}_4 \cdot 3\text{H}_2\text{O}$  ( $0.025 \text{ mol.L}^{-1}$ , 0.005 mmol) was added to a 7.3 mL aqueous solution of surfactant ( $0.0685 \text{ mol.L}^{-1}$ , 0.5 mmol) (except for HEA18Br, a 7.3 mL aqueous solution of surfactant ( $0.0342 \text{ mol.L}^{-1}$ , 0.25 mmol) was used). Then, 0.15 mL of an aqueous solution of silver nitrate ( $4 \times 10^{-3} \text{ mol.L}^{-1}$ ) was

added under stirring, followed by ascorbic acid (0.070 mL, 0.0788 M). The system turned to colorless, proving the reduction of  $\text{Au}^{3+}$  to  $\text{Au}^+$ .

**Growing process:** 0.060 mL of seed particles were added to the freshly prepared growth solution. The solution is kept under stirring for just 10 s and then allowed to stand for 4 h without stirring prior to characterization to ensure the system stability.

## Acknowledgements

This work was supported by the CAPES-COFECUB program Ph/650-10 (PhD grant of M. G. Angelo da Silva and financial support). We thank Patricia Beaunier from Université Pierre et Marie Curie for performing TEM analyses.

## Notes and references

- <sup>75</sup> *Ecole Nationale Supérieure de Chimie de Rennes, CNRS, UMR 6226, 11 Allée de Beaulieu, CS 50837, 35708 Rennes Cedex 7, France.*
- <sup>b</sup> *Grupo de Catálise e Reactividade Química GCaR, Instituto de Química e Biotecnologia da Universidade Federal de Alagoas, Av. Lourival de Melo Mota, s/n CEP 57072-970, Maceió, Brazil.*
- <sup>80</sup> † Electronic Supplementary Information (ESI) available: [details of any supplementary information available should be included here]. See DOI: 10.1039/b000000x/
1. S. Eustis and M. A. El-Sayed, *Chem. Soc. Rev.*, 2006, **35**, 209-217.
- <sup>85</sup> 2. S.-F. Lai, C.-C. Chien, W.-C. Chen, Y.-Y. Chen, C.-H. Wang, Y. Hwu, C. S. Yang and G. Margaritondo, *RSC Adv.*, 2012, **2**, 6185-6191.
3. S. Kumar and T. Nann, *Small*, 2006, **2**, 316-329.
4. R. Sardar, A. M. Funston, P. Mulvaney and R. W. Murray, *Langmuir*, 2009, **25**, 13840-13851.
- <sup>90</sup> 5. K. Rahme, M. T. Nolan, T. Doody, G. P. McGlacken, M. A. Morris, C. O'Driscoll and J. D. Holmes, *RSC Adv.*, 2013, **3**, 21016-21024.
6. B. Lim and Y. Xia, *Angew. Chem., Int. Ed.*, 2011, **50**, 76-85.
7. C. J. Murphy and N. R. Jana, *Adv. Mater. (Weinheim, Ger.)*, 2002, **14**, 80-82.
- <sup>95</sup> 8. S. E. Lohse and C. J. Murphy, *Chem. Mater.*, 2013, **25**, 1250-1261.
9. K. Saha, S. S. Agasti, C. Kim, X. Li and V. M. Rotello, *Chem. Rev. (Washington, DC, U. S.)*, 2012, **112**, 2739-2779.
10. K. Liu, H. Pang, J. Zhang, H. Huang, Q. Liu and Y. Chu, *RSC Adv.*, 2014, **4**, 8415-8420.
- <sup>100</sup> 11. S. H. Radwan and H. M. E. Azzazy, *Expert Rev. Mol. Diagn.*, 2009, **9**, 511-524.
12. L. C. Kennedy, L. R. Bickford, N. A. Lewinski, A. J. Coughlin, Y. Hu, E. S. Day, J. L. West and R. A. Drezek, *Small*, 2011, **7**, 169-183.
- <sup>105</sup> 13. A. M. Alkilany, L. B. Thompson, S. P. Boulos, P. N. Sisco and C. J. Murphy, *Adv. Drug Delivery Rev.*, 2012, **64**, 190-199.
14. M. Eo, J. Baek, H. D. Song, S. Lee and J. Yi, *Chem. Commun. (Cambridge, U. K.)*, 2013, **49**, 5204-5206.
- <sup>110</sup> 15. S. Hebié, L. Cornu, T. W. Napporn, J. Rousseau and B. K. Kokoh, *J. Phys. Chem. C*, 2013, **117**, 9872-9880.
16. L.-F. Zhang and C.-Y. Zhang, *Nanoscale*, 2013, **5**, 5794-5800.
17. J. Xiao and L. Qi, *Nanoscale*, 2011, **3**, 1383-1396.
18. A. R. Tao, S. Habas and P. Yang, *Small*, 2008, **4**, 310-325.
- <sup>115</sup> 19. M. R. Langille, M. L. Personick, J. Zhang and C. A. Mirkin, *J. Am. Chem. Soc.*, 2012, **134**, 14542-14554.
20. Y. Xia, Y. Xiong, B. Lim and S. E. Skrabalak, *Angew. Chem., Int. Ed.*, 2009, **48**, 60-103.
21. M. Grzelczak, J. Perez-Juste, P. Mulvaney and L. M. Liz-Marzan, *Chem. Soc. Rev.*, 2008, **37**, 1783-1791.
- <sup>120</sup> 22. V. R. Dugyala, S. V. Daware and M. G. Basavaraj, *Soft Matter*, 2013, **9**, 6711-6725.
23. B. Nikoobakht and M. A. El-Sayed, *Chem. Mater.*, 2003, **15**, 1957-1962.
- <sup>125</sup> 24. T. K. Sau and C. J. Murphy, *J. Am. Chem. Soc.*, 2004, **126**, 8648-8649.

25. Y. Xiang, X. Wu, D. Liu, L. Feng, K. Zhang, W. Chu, W. Zhou and S. Xie, *J. Phys. Chem. C*, 2008, **112**, 3203-3208.
26. J. E. Millstone, G. S. Métraux and C. A. Mirkin, *Adv. Funct. Mater.*, 2006, **16**, 1209-1214.
- 5 27. J. E. Millstone, W. Wei, M. R. Jones, H. Yoo and C. A. Mirkin, *Nano Lett.*, 2008, **8**, 2526-2529.
28. T. Ming, W. Feng, Q. Tang, F. Wang, L. Sun, J. Wang and C. Yan, *J. Am. Chem. Soc.*, 2009, **131**, 16350-16351.
29. J. Zhang, M. R. Langille, M. L. Personick, K. Zhang, S. Li and C. A. Mirkin, *J. Am. Chem. Soc.*, 2010, **132**, 14012-14014.
- 10 30. Y. Yu, Q. Zhang, X. Lu and J. Y. Lee, *J. Phys. Chem. C*, 2010, **114**, 11119-11126.
31. M. G. A. da Silva, Á. M. Nunes, S. M. P. Meneghetti and M. R. Meneghetti, *C. R. Chimie*, 2013, **16**, 640-650.
- 15 32. J. Gao, C. M. Bender and C. J. Murphy, *Langmuir*, 2003, **19**, 9065-9070.
33. H. Kawasaki, K. Nishimura and R. Arakawa, *J. Phys. Chem. C*, 2007, **111**, 2683-2690.
34. S. E. Lohse, N. D. Burrows, L. Scarabelli, L. M. Liz-Marzán and C. J. Murphy, *Chem. Mater.* 2014, **26**, 34-43.
- 20 35. X. Kou, S. Zhang, C.-K. Tsung, M. H. Yeung, Q. Shi, G. D. Stucky, L. Sun, J. Wang and C. Yan, *J. Phys. Chem. B*, 2006, **110**, 16377-16383.
36. X. Kou, S. Zhang, C.-K. Tsung, Z. Yang, M. H. Yeung, G. D. Stucky, L. Sun, J. Wang and C. Yan, *Chem.--Eur. J.*, 2007, **13**, 2929-2936.
- 25 37. M. G. A. da Silva, M. R. Meneghetti, A. Denicourt-Nowicki and A. Roucoux, *RSC Adv.*, 2013, **3**, 18292-18295.
38. J. Schulz, A. Roucoux and H. Patin, *Chem.--Eur. J.*, 2000, **6**, 618-624.
- 30 39. A. Roucoux, J. Schulz and H. Patin, *Adv. Synth. Catal.*, 2003, **345**, 222-229.
40. E. Guyonnet Bile, R. Sassine, A. Denicourt-Nowicki, F. Launay and A. Roucoux, *Dalton Trans.*, 2011, **40**, 6524-6531.
- 35 41. T. K. Sau and C. J. Murphy, *Langmuir*, 2004, **20**, 6414-6420.
42. X. Xu and M. B. Cortie, *Adv. Funct. Mater.*, 2006, **16**, 2170-2176.
43. J. Pérez-Juste, L. M. Liz-Marzán, S. Carnie, D. Y. C. Chan and P. Mulvaney, *Adv. Funct. Mater.*, 2004, **14**, 571-579.
44. T. H. Ha, H.-J. Koo and B. H. Chung, *J. Phys. Chem. C*, 2007, **111**, 1123-1130.
- 40 45. G. Cerichelli, L. Luchetti, G. Mancini and G. Savelli, *Tetrahedron*, 1995, **51**, 10281-10288.
46. V. Sharma, K. Park and M. Srinivasarao, *Mater. Sci. Eng., R*, 2009, **65**, 1-38.
- 45 47. O. M. Magnussen, *Chem. Rev. (Washington, DC, U. S.)*, 2002, **102**, 679-725.
48. D. K. Smith, N. R. Miller and B. A. Korgel, *Langmuir*, 2009, **25**, 9518-9524.
49. Doori Lee, Soonchang Hong and S. Park, *Bull. Korean Chem. Soc.*, 2011, **32**, 3575-3580.
- 50 50. Z. Guo, X. Fan, L. Liu, Z. Bian, C. Gu, Y. Zhang, N. Gu, D. Yang and J. Zhang, *J. Colloid Interface Sci.*, 2010, **348**, 29-36.

55

## Graphical Abstract

Size- and shape-controlled anisotropic gold nanoparticles were reported. The organisation of tunable hydroxylated surfactants providing various nanostructured materials has been demonstrated.

